

# Strömgren four-color photometry of X-ray active late-type stars: Evidence for activity-induced deficiency in the $m_1$ index<sup>\*</sup>

F. Morale<sup>1</sup>, G. Micela<sup>1</sup>, F. Favata<sup>2</sup> and S. Sciortino<sup>1</sup>

<sup>1</sup> Istituto e Osservatorio Astronomico di Palermo, Palazzo dei Normanni, 90134 Palermo, Italy

<sup>2</sup> Astrophysics Division, European Space Agency – Postbus 299, 2200 AG Noordwijk, The Netherlands

Received October 30, 1995; accepted February 9, 1996

**Abstract.** — We present the results of a *wby*- $\beta$  photometric study of a sample of active late-type stars (F–K) selected from the *Einstein* Extended Medium Sensitivity Survey. Our work shows the presence in the sample of a star population with the photometric index  $c_1$  typical of main sequence stars and an unexpected deficiency in  $m_1$  index. Stars with more anomalous values of  $m_1$  have also very high values of  $f_X/f_V$  and X-ray surface fluxes, near the “saturation” limit observed in the most active stars and similar to the flux observed in solar active regions. We discuss these results in the light of similar results found in the Sun comparing  $m_1$  indices in quiet and active regions and in other samples of active stars.

**Key words:** stars: activity — stars: late-type — stars: abundances — X-rays: stars

## 1. Introduction

X-ray flux limited surveys have been a very powerful medium for the study of the characteristics of known populations of coronal emitters, as well as for the discovery of new populations with unremarkable optical characteristics, which would therefore be difficult to detect otherwise. One of the most productive surveys has been the *Extended Medium Sensitivity Survey* (EMSS, Gioia et al. 1990), an X-ray flux limited survey based on data acquired with the Imaging Proportional Counter on board the *Einstein* observatory, which constitutes to date the largest published unbiased and essentially fully identified sample of X-ray sources.

By comparing the contents of the EMSS with expected source counts based on Galaxy models Favata et al. (1988) and Sciortino et al. (1995) have shown the existence of an excess population of yellow stars in the EMSS with respect to the source counts expected for normal main sequence stars. Favata et al. (1993, 1995), studying the optical counterparts, have shown that this excess is largely due to a young (i.e. with an age close to ZAMS) stellar population which appears to be under-represented in the solar neighborhood. A similar conclusion has been reached by Tagliaferri et al. (1994) studying the High Latitude X-ray EXOSAT survey. Also, Jeffries & Bromage (1993)

and Hodgkin & Pye (1994) have studied the excess of EUV sources they found by comparing EUV luminosity functions deduced from ROSAT WFC observations of nearby stellar sources with the  $\log(N)$ – $\log(S)$  derived from the EUV Bright Source Catalog (Pounds et al. 1993), reaching similar conclusions.

To further investigate the nature of the solar-type stellar populations in the EMSS a photometric campaign in the Strömgren-Crawford *wby*- $\beta$  system was performed, on a sample of EMSS sources, at the same time as the spectroscopic observations reported by Favata et al. (1993). The original primary aim of these observations was to determine effective temperatures and luminosity classes for the observed sources. In addition to fulfilling this aim, a detailed study of the  $m_1$  color index in our sample has allowed us to explore the effect of activity on the “traditional” metallicity photometric indicator  $m_1$ , which had already been shown to deviate from the expected behavior in samples of very active stars (see for example Giménez et al. 1991).

Strömgren photometry has been a very powerful tool for the investigation of several important questions about stellar populations and Galactic stellar structure. Following the large body of observational work on early type stars (from B to early G), which has yielded important calibrations of fundamental astrophysical quantities (Crawford 1975, 1978, 1979; Nissen 1981; McNamara & Powell 1985; Saxner & Hammarbäck 1985; Olsen 1988; Nissen & Schuster 1991), more recently a large effort

Send offprint requests to: F. Morale

<sup>\*</sup>Based on observations collected at the ESO La Silla observatory

has been directed toward enlarging the applicability of the calibrations toward later type stars (Ardeberg & Lindgren 1981; Olsen 1984; Ardeberg & Lindgren 1985; Reglero et al. 1990). We have fruitfully tapped into this large body of recent work for the analysis presented here.

The present paper is organized as follows: in Sect. 2 we describe the observed sample, in Sect. 3 we present the observations and the data reduction and analysis, in Sect. 4 we present our results, and in Sect. 5 we discuss our findings, in particular the meaning of the  $m_1$  color in very active stars. Our main conclusions are summarized in Sect. 6.

## 2. Program stars

The sample discussed in the present paper is composed of 49 yellow stars selected from the coronal sources detected in the EMSS. They were selected in the color range  $B - V$  comprised between 0.4 and 1.4 and are brighter than  $V$  magnitude  $\approx 12$ . Apart from the color and magnitude cuts, the only additional selection criterion imposed on the sample has been the visibility, i.e. the stars in the sample were visible from the ESO La Silla observatory, with the Danish 50 cm (*Strömgren Automatic Telescope*, SAT) during the observational campaign (August 1991). All the stars in the sample have measured X-ray fluxes from the EMSS, and a large fraction of them (32 out of 49) have had their lithium abundances and rotational velocities spectroscopically determined in the course of the same observational campaign (Favata et al. 1993). Additionally, several of the sample stars (22) have been studied by searching for companions through radial velocity measurements (Fleming 1989; Stocke 1991; Baker et al. 1994). Table 1 summarizes the main known characteristics of the program stars.

As expected given the nature of the selection bias imposed by X-ray flux limited survey, our sample is dominated by very active stars, on the high luminosity tail of the X-ray luminosity distribution.

## 3. Observations and data reduction

### 3.1. Observations

All the measurements presented here were obtained with the SAT telescope at the ESO La Silla observatory. The SAT is a 0.50 m Cassegrain telescope, devoted to  $uvby$  and  $\beta$  photoelectric photometry, with computer programmed capabilities for the automatic execution of the observation program (Olsen 1994). The photometer is a six channel, microprocessor controlled instrument, and has dead time constants of 72, 95, 88 and 73 ns for the  $u, v, b, y$  channels, of 71 ns for the  $H\beta N$  channel, and of 89 ns for the  $H\beta W$  channel (Schwarz & Melnick 1989).

The data discussed here were collected during seven nights in the first week of August 1991, using a 17 arcsec

diaphragm for both the  $uvby$  and the  $\beta$  channels. The integration time for program stars was chosen to obtain, for stars to  $V = 10$  (corresponding to the bulk of our sample) a  $S/N$  ratio of 100 in the photometer  $u$  and  $\beta$  channels. The  $S/N$  is usually higher in the other channels.

The rate of standard star ( $uvby$  and  $\beta$ ) measurements was of 4 or 5 per hour, and some of those stars were observed in  $uvby$  up to an airmass 2, to measure atmospheric extinction effects during the night. The sky background was observed after every star, both for the  $uvby$  and the  $\beta$  measurements.

### 3.2. $uvby$ data reduction

We have analyzed the data in two steps: first we have computed the instrumental catalog, determining the various instrumental and observational factors that contribute to the results, and then we transformed the data to the Crawford-Barnes (1970) standard values.

First of all, to obtain the extra-atmospheric magnitude and colors for standard stars, we have minimized a multi-night, multi-star merit function, with time drift terms and extinction coefficients, built according to the suggestions of Manfroid & Heck (1983) and Sterken & Manfroid (1992), fixing at least a mean term to roughly reduce our catalog to standard values. We then reduced this preliminary flexure-dependent instrumental catalog to the standard values listed in Table 8 of Olsen (1993) through Crawford & Barnes (1970) expressions, modified to take into account the instrumental flexure errors. (the NOAO-IRAF *fitparams* task was mostly used for the purpose). The flexure coefficients determined here, shown in Table 2, are different from the values of Olsen (1993, 1994), while the other transformation coefficients are very similar to the values of Olsen (1993).

After applying the flexure correction to the magnitude ( $y$ ) and to the color data, we have used the corrected values to recompute the merit function and to finally derive our instrumental catalog for the SAT in August 1991, as shown in Table 3.

A comparison between our catalog and Olsen's (1993) does not reveal systematic effects, with the exception of a small zero point shift. Therefore we are confident that the SAT instrument did not undergo substantial changes between 1987 (the date of Olsen's observations) and 1991. The root mean squares (RMS) residuals are 0.007, 0.004, 0.006, 0.007, 0.004 for  $y$ ,  $(b-y)$ ,  $m_1$ ,  $c_1$  and  $\beta$ , respectively.

In the transformation from instrumental to standard values a crucial step is the dependence on color that, for Strömgren photometry, is different for early and late type stars and among late type stars is furthermore different for main sequence and giants stars (Gronbech et al. 1976; Olsen 1983, 1984, 1993, 1994; Sterken & Manfroid 1992).

Taking advantage of the good agreement between our and Olsen's (1993) instrumental catalogs and of the similarity between our transformation coefficients (determined

**Table 1.** Optical characteristics of program stars

#	EMSS Name	Other name	$V^1$	Spec. type <sup>1</sup>	$\log n(\text{Li})^2$	$v\text{-sin}i^3$ (km/s)	Binary?
1	MS0002.8+1602	HD 42	8.6	F5V	2.50	11	B
2	MS0003.3-4201	HD 105	7.4	G0V	3.40	13	
3	MS0009.9+1417	BD+13 13	8.5	G5V	1.35	25	B
4	MS0031.9-0646	HD 3126	6.8	F4V	2.95	27	
5	MS0138.0-5627	HD 10360/10361	5.8	K5V/K0V	-0.95	11	B
6	MS0206.2-1019		8.9	G5V	0.95	19	
7	MS0234.2-0321	HD 16287	8.1	K2V	-0.05	11	B?
8	MS0234.7-0210		10.4	G9V	1.00	10	
9	MS0236.4-0148	HD 16525	9.0	F8V	2.25		B?
10	MS0244.8-0024	BD-00431	9.6	G9V	1.10	$\leq 8$	B
11	MS0300.1-1528	HD 18955	8.4	G8V	0.50	20	B?
12	MS0318.5-1926		10.8	K7V	1.05	17	
13	MS0324.1-2012		10.5	G4V			
14	MS0326.6-2008	BD-20 646	10.1	F4V	2.90	15	B?
15	MS0327.2-2416	HD 21703	9.1	K7V		14	
16	MS0333.1+0607		10.3	F6V	3.10	33	
17	MS0337.6-0202	HD 22853	8.0	G9V	1.20	18	
18	MS0348.2-1404		10.7	K0IV	1.95	$\leq 8$	B?
19	MS0356.9+1011	HD 25102	6.4	F5V			
20	MS0420.3-3900		12.0	F6V			
21	MS0438.5+0213		10.6	F9V	0.65	48	B?
22	MS0452.2+0225		10.6	K0V	1.40	$\leq 8$	B?
23	MS0457.5+0312	HD 25102	7.5	K2V	2.05	37	
24	MS0515.4-0710		10.8	K2e	2.70	11	
25	MS1247.0-0548	HD 111487	9.7	G5			B
26	MS1254.8+0142	HD 112542	7.0	F4V	2.40	28	
27	MS1330.5-0811	HD 117860	7.2	G0V	2.55	$\leq 8$	
28	MS1335.9-2918	HD 118646	5.8	F5V			
29	MS1428.2+0732		11.0	F7V			B?
30	MS1436.8-2628	SAO 182743	9.7	K4V	-0.05	10	B?
31	MS1457.0+2108		11.1	F8V			
32	MS1520.2+2548	HD 136901	7.4	K1III			B
33	MS1528.5+0844	HD 138290	6.5	F4V			B?
34	MS1533.0+0919		11.7	K4Ve			
35	MS1552.0-2338	HD 142361	8.8	G3IV	4.05	53	
36	MS1558.4-2232		11.4	K3e	3.10	$\leq 8$	
37	MS1559.2-2232		11.3	K5e			B?
38	MS1753.5+1830	GJ 698	9.2	K4	0.75	$\leq 8$	B?
39	MS1758.9+2339		10.7	K3V			
40	MS1907.0-6405		11.8	K4V	0.05	21	
41	MS2038.3-0046	HD 197010	9.3	F8V			B?
42	MS2119.7+1655		11.7	F6V			B?
43	MS2125.5-1503		11.4	F8V			B?
44	MS2148.2+1420		11.4	K3IV/V	1.60	$\leq 8$	B?
45	MS2254.2+0219		10.2	K2V	1.15	43	
46	MS2302.4-4427	HD 218033	9.7	G8	1.25	16	
47	MS2315.1-3640		11.3	K2V/K4V		12	
48	MS2335.2+0305	HD 222111	7.3	F5V	1.75	11	
49	MS2349.8-0112		10.7	K0III	3.75	64	

<sup>1</sup> Data from Stocke et al. (1991); <sup>2</sup> Data from Favata et al. (1993); <sup>3</sup> Data from Favata et al. (1995).

in the course of the determination of flexure effects) and Olsen's (1993), we have decided to use the transformation of Olsen, which was obtained by using a larger number of standard stars than ours, after adding a zero point correction of few millimagnitudes to our instrumental catalogue, in order to match the values reported in Table 3 of Olsen (1993).

All the transformations determined by the reduction process described above were applied to the program stars together with the color transformation based on the deci-

sion procedure described in Fig. 1 of Olsen (1993), which has made possible to perform a luminosity classification on the basis of the instrumental colours ( $b - y$ ) and  $c_1$ .

The catalogue of standard stars reduced to the Crawford-Barnes standard values is shown in Table 4. The standard values of program stars are listed in Table 5<sup>1</sup>,

<sup>1</sup>On June 15 1991, some weeks before our observations, the Pinatubo volcano ( $\approx +15^\circ$  latitude), in the Philippines, underwent an explosive eruption launching a great mass of ashes and gases in atmosphere. Effects of volcano eruptions

where the number of observations in the  $y$  channel,  $n_y$ , and of observations for the colors,  $n_{uvb}$ , can be different because some non-photometric parts of nights, which are not usable for magnitude determinations, are however usable for color measurements when using a simultaneous data collecting photometer like the SAT (cf. Olsen 1983, 1993; Schuster & Nissen 1988).

**Table 2.** Flexure coefficients for the gradient in declination ( $\delta$ ) and in hour angle ( $h$ ). Values and errors are the result of a minimization procedure. The correction to be applied to an observed index is  $-K\delta$  and  $-Lh$

$K(y)$ mag/rad	$K(b-y)$ mag/rad	$K(m_1)$ mag/rad	$K(c_1)$ mag/rad	$K(\beta)$ mag/rad
-0.0117 $\pm 0.0013$	+0.0030 $\pm 0.0009$	-0.0017 $\pm 0.0011$	+0.0075 $\pm 0.0017$	-0.0061 $\pm 0.0030$
$L(y)$ mag/hour	$L(b-y)$ mag/hour	$L(m_1)$ mag/hour	$L(c_1)$ mag/hour	$L(\beta)$ mag/hour
+0.00011 $\pm 0.00005$	-0.00006 $\pm 0.00004$	+0.00002 $\pm 0.00004$	+0.00024 $\pm 0.00006$	0.00008 $\pm 0.00013$

### 3.3. The $\beta$ data reduction

To reduce  $\beta$  data we followed the same procedure described above for the  $uvby$  data: we first minimized a merit function, similar to that adopted for  $uvby$  measurements but without the extinction term and we then built a preliminary instrumental catalog forcing the data to Crawford-Mander standard values. In the expressions for the reduction to the standard system (Crawford & Mander 1966) we introduced two terms, one for the hour angle and another for the declination, to correct for the flexure error. The corrected data were used as input to compute the final instrumental catalog, shown in Table 3, again by minimizing the merit function. It is known that the  $\beta$  transformation to the standard is different for B–A stars and for A–G; the transformation to the standard values (Perry et al. 1987) of our stars were made forcing all the stars with parameters computed for A–G stars because our sample includes only late-type stars. In Tables 4 and 5 we show standard  $\beta$  values for standard and program stars respectively.

on atmospheric extinction have been well studied in relation with photometric observations (Rufener 1986; Grothues & Gochermann 1992; Manfroid 1992). Results of these studies pointed out that a color dependent increase of the extinction coefficients as well as a great variability of the coefficients can be measured after eruptions, with effects slowly decreasing in the months following the explosion. These effects appear after a time strongly dependent on the geographical coordinates of the site of eruption and of the site of observation, as well as on meteorological factors. Our efforts to search for effects of the Pinatubo eruption in our data produced no results, justifying our choice of a single extinction coefficient per night.

Typical standard deviations for stars with  $V \leq 10$  are 0.01, 0.01, 0.01, 0.015 and 0.02 for  $V$ ,  $(b-y)$ ,  $m_1$ ,  $c_1$  and  $\beta$  respectively; for fainter stars a value of 0.03 is a realistic evaluation of the uncertainty of the data for all colors. Some very large values of the standard deviation, specially in  $V$ , was found for some binary systems, indicating possible variability.

## 4. Results

Figures 1a and 1b show plots of  $c_1$  and  $m_1$  vs.  $b-y$  for our program stars. Continuous lines indicate the standard main sequence for F (Crawford 1975) and G–M (Olsen 1984) stars. The dashed line connects data obtained by Perry et al. (1987) for 13 class III stars; this line shows the region populated by metal rich giants (Ardeberg & Lindgren 1981). The stars we have used to define the class III region are reported in Table 6 together with their [Fe/H] abundance (Cayrel de Strobel et al. 1992). We have assumed that the effects of interstellar reddening are negligible because, given the typical sensitivity of *Einstein* X-ray observations and the activity level of a very young star, all the EMSS coronal sources should lie at a distance of 100 pc or less, as it is in fact confirmed by the photometric parallax of the stars in our sample, as well as by the good agreement we find between their  $b-y$  and  $\beta$  indices. As discussed earlier, the luminosity class of the sample stars was determined during the transformation to the standard values, using the  $(b-y)$  and  $c_1$  indices. The spectral types classification was performed using the  $\beta$  and  $(b-y)$  indices for F dwarfs, following Crawford (1975, Table VII), and the  $(b-y)$  index alone for G–K dwarf, following Olsen (1984, Tables V and VI). For class III stars, the  $(b-y)$  index was used irrespective of spectral type, following Ardeberg & Lindgren (1985, Fig. 2). The diagram shown in panel (a) of Fig. 1 allows us to clearly separate dwarfs from giants. Note that we have classified as class III some stars having a very high lithium abundance, close to the typical “primordial” value for Pop. I objects, which are unlikely to be evolved objects, and are much more likely to be pre-main sequence objects.

The  $m_1$  vs.  $b-y$  diagram of Fig. 1b is normally used to estimate the stellar metallicity by measuring the quantity  $\delta m_1$ , defined as  $m_{1(\text{Hyades})} - m_{1(\text{obs})}$ . Inspection of Fig. 1b shows that most of the cooler stars (both dwarfs and giants) in our sample have  $m_1$  values which are typical of metal poor stars. Some of the main sequence stars in the sample have a  $\delta m_1$  value large enough to position them in the region normally occupied by giants.

From Fig. 1b it is evident that the deviation from the standard solar-metallicity sequence for the stars in our sample has a definite color dependence. This is better shown in Fig. 2, where the quantity  $\delta m_{1(b-y)}$ , defined according to Crawford (1975) as  $m_{1,\text{standard}} - m_{1,\text{star}}$  is plotted versus the color index  $b-y$ . Different symbols identify stars of different luminosity class, as determined from the

**Table 3.** Instrumental catalog for the SAT in August 1991. The number of observations used in the minimization phases for each color is  $n$ ;  $\text{Res}_{\text{index}} = \sum_i (\text{res}_i)^2 / (i - 1)$  where  $i$  is the running index of the observations

Name	$y$	$n$	$b - y$	$n$	$m_1$	$n$	$c_1$	$n$	$\beta$	$n$	$\text{Res}_V$	$\text{Res}_{b-y}$	$\text{Res}_{m_1}$	$\text{Res}_{c_1}$	$\text{Res}_\beta$
HR100	3.959	18	0.091	18	0.202	18	0.944	16	2.815	5	0.009	0.005	0.004	0.006	0.006
HR531	4.651	6	0.212	9	0.184	9	0.661	7	2.737	6	0.007	0.005	0.005	0.009	0.012
HR672	5.604	6	0.371	6	0.178	6	0.417	6	2.646	1	0.008	0.006	0.007	0.008	–
HR962	5.066	6	0.362	9	0.173	9	0.430	8	–	–	0.005	0.004	0.006	0.007	–
HR1024	6.208	6	0.449	12	0.189	12	0.312	7	–	–	0.004	0.004	0.004	0.008	–
HR1089	6.484	9	0.412	12	0.173	12	0.452	10	2.648	7	0.005	0.004	0.005	0.009	0.010
HR1552	3.690	3	-0.043	3	0.062	3	0.198	3	–	–	0.013	0.004	0.006	0.005	–
HR2106	–	–	–	–	–	–	–	–	2.644	3	–	–	–	–	0.010
HR4695	4.959	3	0.713	3	0.504	3	0.354	3	–	–	0.006	0.004	0.006	0.008	–
HR5168	4.237	15	0.246	15	0.168	15	0.554	15	2.705	6	0.006	0.005	0.006	0.007	0.005
HR5511	3.742	12	0.006	12	0.144	12	1.112	11	2.818	6	0.009	0.005	0.007	0.008	0.007
HR5530	5.158	12	0.270	12	0.150	12	0.518	12	2.697	6	0.005	0.005	0.008	0.009	0.007
HR5660	4.920	15	0.249	16	0.133	16	1.374	16	2.738	4	0.006	0.004	0.006	0.009	0.005
HR5868	4.419	13	0.384	13	0.184	13	0.374	13	2.636	4	0.008	0.004	0.006	0.008	0.008
HR5997	4.317	16	0.514	16	0.301	16	0.381	14	2.615	4	0.007	0.004	0.006	0.006	0.011
HR6332	–	–	–	–	–	–	–	–	2.855	6	–	–	–	–	0.011
HR6458	–	–	–	–	–	–	–	–	2.624	6	–	–	–	–	0.010
HR6723	4.443	18	0.036	18	0.133	18	1.128	18	2.831	6	0.008	0.005	0.006	0.005	0.009
HR7254	4.117	13	0.024	13	0.181	13	1.091	14	2.854	6	0.008	0.004	0.006	0.007	0.011
HR7858	5.391	13	0.027	13	0.201	13	1.023	12	2.877	4	0.007	0.006	0.008	0.008	0.004
HR8060	4.859	19	0.089	19	0.190	19	0.983	19	2.826	6	0.005	0.004	0.006	0.007	0.010
HR8313	4.305	10	0.699	10	0.513	10	0.202	10	–	–	0.007	0.004	0.004	0.004	–
HR8431	4.504	1	0.031	1	0.169	1	1.105	1	–	–	–	–	–	–	–
HR8729	5.446	4	0.415	4	0.215	4	0.374	4	–	–	0.009	0.006	0.006	0.008	–
HR8848	4.012	19	0.264	19	0.154	19	0.560	19	2.669	5	0.009	0.003	0.006	0.008	0.010
HR8969	4.129	9	0.333	9	0.156	9	0.413	9	2.644	6	0.008	0.005	0.008	0.008	0.011

**Table 4.** Mean values and standard deviations for standard stars in the Crawford-Barnes ( $uvby$ ) and Crawford-Mander ( $\beta$ ) systems. An asterisk in column 12 (Notes) indicates stars which are not  $\beta$  standards. The few B stars present in Table 3 only with  $\beta$  values are not reported here because an A–F transformation to standard was applied to all stars

Name	$V$	$b - y$	$m_1$	$c_1$	$\beta$	$\sigma_V$	$\sigma_{b-y}$	$\sigma_{m_1}$	$\sigma_{c_1}$	$\sigma_\beta$	Notes
HR100	3.942	0.088	0.205	0.912	2.846	0.011	0.005	0.006	0.005	0.008	
HR531	4.650	0.209	0.188	0.641	2.741	0.008	0.006	0.008	0.010	0.015	
HR672	5.609	0.372	0.179	0.413	2.623	0.008	0.007	0.011	0.005	–	
HR962	5.075	0.363	0.180	0.421	2.627	0.013	0.003	0.003	0.007	0.026	*
HR1024	6.212	0.448	0.203	0.301	2.571	0.004	0.004	0.008	0.009	0.018	*
HR1089	6.493	0.410	0.188	0.444	2.627	0.005	0.003	0.005	0.009	0.013	
HR1552	3.688	-0.052	0.069	0.141	–	0.013	0.004	0.006	0.005	–	
HR4695	4.971	0.721	0.472	0.502	2.560	0.003	0.001	0.006	0.007	0.015	*
HR5168	4.221	0.246	0.172	0.534	2.702	0.007	0.005	0.006	0.009	0.006	
HR5511	3.737	-0.004	0.150	1.074	2.841	0.011	0.004	0.007	0.008	0.009	
HR5530	5.149	0.266	0.157	0.500	2.689	0.005	0.005	0.009	0.009	0.009	
HR5660	4.925	0.246	0.141	1.367	2.744	0.025	0.005	0.006	0.010	0.006	
HR5868	4.427	0.380	0.192	0.366	2.607	0.008	0.005	0.007	0.008	0.010	
HR5997	4.314	0.522	0.282	0.453	2.584	0.007	0.004	0.006	0.005	0.014	
HR6723	4.436	0.026	0.140	1.093	2.857	0.013	0.005	0.007	0.006	0.013	
HR7254	4.096	0.020	0.185	1.056	2.896	0.009	0.003	0.006	0.007	0.014	
HR7858	5.389	0.019	0.203	0.989	2.917	0.010	0.006	0.008	0.008	0.005	
HR8060	4.857	0.084	0.193	0.953	2.856	0.012	0.004	0.005	0.007	0.013	
HR8313	4.328	0.703	0.483	0.358	2.606	0.007	0.003	0.003	0.008	0.023	*
HR8431	4.489	0.028	0.172	1.070	–	–	–	–	–	–	
HR8729	5.456	0.411	0.239	0.363	2.606	0.004	0.005	0.004	0.010	0.029	*
HR8848	3.991	0.267	0.158	0.543	2.661	0.012	0.004	0.006	0.008	0.012	
HR8969	4.135	0.328	0.165	0.400	2.620	0.008	0.004	0.004	0.009	0.014	

analysis of the  $c_1$  index. The dashed line indicates the expected  $\delta m_1$  value of giants with respect to the main sequence. Note that some stars have a  $\delta m_1$  comparable with that observed in halo stars (Olsen 1984; Schuster & Nissen 1989); given that most other characteristics of the EMSS coronal source population point toward it being mostly composed of young (i.e. close to ZAMS) sources (Favata et al. 1993, 1995), the large metal deficiency implied by the  $m_1$  index taken at face value seems very unlikely.

## 5. Discussion

Given the magnitude of the observed  $\delta m_1$  in our sample of stars and their belonging to a young, active population, the observed behavior cannot be entirely explained in terms of a real metal deficiency. The dependence of the  $m_1$  deficiency on the effective temperature seems to indicate a real peculiarity of the atmospheres of our active stars with respect to “normal” stars, similar to that observed in active binaries by Giménez et al. (1991). These

**Table 5.** Spectral type, derived by photometry discussed in the text, and mean values and standard deviations for program stars in the Crawford & Barnes (*uvby*) and Crawford & Mander ( $\beta$ ) systems. The number of observations for the *V* magnitude and colors are  $n_y$  and  $n_{uvb}$ , respectively. A 9.999 in the  $\sigma$  columns indicates stars with only one observation

N.	Sp. Type	<i>V</i>	$n_y$	<i>b</i> - <i>y</i>	$m_1$	$c_1$	$n_{uvb}$	$\beta$	$n_\beta$	$\sigma_V$	$\sigma_{b-y}$	$\sigma_{m_1}$	$\sigma_{c_1}$	$\sigma_\beta$
1	F5V	8.620	6	0.291	0.148	0.460	6	2.663	6	0.008	0.008	0.009	0.011	0.022
2	G0V	7.500	15	0.371	0.182	0.312	15	2.607	6	0.106	0.007	0.009	0.010	0.021
3	K0V	8.454	9	0.479	0.251	0.268	9	2.575	6	0.030	0.008	0.009	0.011	0.009
4	F5V	6.910	12	0.304	0.151	0.393	12	2.649	6	0.014	0.005	0.006	0.009	0.018
5	K3V	5.619	6	0.504	0.397	0.256	6	2.527	6	0.163	0.005	0.009	0.015	0.023
6	G8V	8.916	6	0.453	0.248	0.275	9	2.577	6	0.010	0.005	0.007	0.013	0.024
7	K2V	8.100	3	0.535	0.484	0.263	3	2.563	3	0.003	0.001	0.005	0.008	0.010
8	G0III	10.310	3	0.473	0.275	0.403	3	–	–	0.019	0.006	0.010	0.017	–
9	F8V	8.916	3	0.350	0.156	0.377	3	2.611	3	0.006	0.001	0.006	0.010	0.020
10	K1V	9.626	3	0.492	0.270	0.277	3	–	–	0.001	0.006	0.011	0.007	–
11	K0V	8.442	3	0.489	0.329	0.320	6	2.581	6	0.006	0.008	0.009	0.009	0.013
12	K5V	10.312	3	0.635	0.549	0.197	3	–	–	0.007	0.006	0.006	0.021	–
13	G5V	10.504	3	0.417	0.216	0.298	6	2.583	3	0.007	0.009	0.017	0.037	0.022
14	F7V	10.133	3	0.337	0.164	0.421	6	2.638	6	0.006	0.007	0.011	0.016	0.031
15	K4V	9.143	3	0.627	0.554	0.152	6	2.508	6	0.001	0.007	0.008	0.019	0.023
16	F7V	10.314	3	0.356	0.136	0.431	6	2.650	3	0.002	0.011	0.021	0.017	0.053
17	K0III	7.287	6	0.684	0.440	0.384	6	2.562	6	0.001	0.004	0.004	0.009	0.032
18	K2IV	10.656	6	0.516	0.268	0.318	6	2.575	3	0.043	0.013	0.020	0.022	0.025
19	F5V	6.346	6	0.276	0.163	0.492	6	2.693	3	0.005	0.004	0.005	0.007	0.020
20	F6V	12.059	3	0.320	0.131	0.430	3	–	–	0.012	0.004	0.014	0.017	–
21	G8III	10.645	3	0.584	0.141	0.428	6	–	–	0.003	0.005	0.010	0.021	–
22	K1V	10.485	3	0.491	0.281	0.258	3	–	–	0.004	0.003	0.010	0.020	–
23	K2III	7.469	3	0.805	0.523	0.322	3	–	–	0.001	0.002	0.002	0.008	–
24	K0III	10.770	3	0.640	0.260	0.488	3	–	–	0.007	0.049	0.019	0.068	–
25	G8V	9.732	30	0.456	0.231	0.266	30	2.568	6	0.184	0.010	0.011	0.018	0.021
26	F5V	6.913	12	0.289	0.169	0.472	12	2.660	6	0.006	0.006	0.007	0.009	0.029
27	G2V	7.358	15	0.392	0.206	0.329	15	2.584	6	0.015	0.005	0.009	0.010	0.032
28	F4V	5.818	15	0.268	0.169	0.540	15	2.682	6	0.009	0.005	0.007	0.009	0.040
29	G3V-IV	10.953	9	0.409	0.175	0.365	9	2.619	3	0.013	0.007	0.009	0.035	0.023
30	K4V	9.737	12	0.605	0.554	0.194	30	2.548	3	0.009	0.008	0.009	0.015	0.032
31	G0V	11.185	3	0.371	0.134	0.398	3	–	–	0.017	0.015	0.014	0.011	–
32	K0III	7.333	13	0.651	0.335	0.422	13	2.549	6	0.029	0.005	0.005	0.012	0.019
33	F2V	6.584	10	0.239	0.158	0.506	10	2.696	3	0.022	0.006	0.006	0.010	0.023
34	K1III	8.101	1	0.745	0.491	0.398	1	–	–	9.999	9.999	9.999	9.999	–
35	G6V-IV	8.935	16	0.438	0.210	0.311	16	2.588	6	0.014	0.006	0.009	0.015	0.024
36	K0III	11.424	7	0.704	0.356	0.348	7	–	–	0.022	0.013	0.019	0.043	–
37	K1III	11.278	4	0.728	0.414	0.324	4	–	–	0.006	0.007	0.018	0.020	–
38	K5V	9.154	12	0.666	0.722	0.115	12	2.521	6	0.009	0.005	0.010	0.020	0.018
39	K0III	10.535	6	0.657	0.303	0.376	6	2.578	6	0.019	0.012	0.015	0.033	0.034
40	K5V	11.803	7	0.628	0.385	0.178	7	–	–	0.022	0.013	0.030	0.049	–
41	G2V	9.094	15	0.396	0.163	0.348	15	2.619	6	0.018	0.004	0.009	0.014	0.006
42	G2V-IV	11.579	9	0.386	0.164	0.396	9	–	–	0.052	0.022	0.023	0.019	–
43	F6V	11.444	13	0.329	0.146	0.396	13	–	–	0.015	0.016	0.023	0.026	–
44	K3V	11.418	1	0.581	0.415	0.172	1	–	–	9.999	9.999	9.999	9.999	–
45	G8III	10.263	19	0.576	0.203	0.439	19	2.616	6	0.035	0.013	0.014	0.029	0.035
46	G8V	9.842	19	0.454	0.222	0.286	19	2.563	6	0.018	0.010	0.012	0.009	0.017
47	K2V	11.366	4	0.514	0.321	0.214	4	–	–	0.081	0.006	0.014	0.038	–
48	F4V	7.295	10	0.295	0.161	0.487	10	2.686	6	0.008	0.004	0.008	0.009	0.012
49	G4V	10.679	6	0.432	0.205	0.296	6	2.608	3	0.019	0.007	0.004	0.027	0.020

**Table 6.** Standard *uvby* values (Perry et al. 1987) and [Fe/H] (Cayrel de Strobel et al. 1992) abundances for the class III sequence

Name	Sp. Type	<i>V</i>	<i>b</i> - <i>y</i>	$m_1$	$c_1$	[Fe/H]
HR8665	F6III-IV	4.190	0.330	0.147	0.407	-0.05/ - 0.28
HR2662	G0III-IV	6.294	0.359	0.192	0.402	
HR3815	G8III	5.410	0.473	0.304	0.372	0.00
HR5997	G3II-III	4.316	0.522	0.285	0.448	
HR1030	G6III	3.613	0.547	0.333	0.426	
HR2985	G8III	3.570	0.573	0.379	0.398	
HR1373	K0III	3.759	0.597	0.424	0.405	
HR4392	G7.5III	4.989	0.610	0.416	0.396	+0.06
HR617	K2IIIab	2.000	0.696	0.526	0.395	-0.21/ - 0.08/ - 0.25/ - 0.29
HR6603	K2III	2.760	0.719	0.553	0.451	+0.14
HR5947	K2IIIab	4.150	0.751	0.570	0.414	
HR3003	K5III	4.848	0.895	0.735	0.451	
HR1457	K5III	0.860	0.955	0.814	0.373	0.00/ - 0.10/ - 0.33/ - 0.14

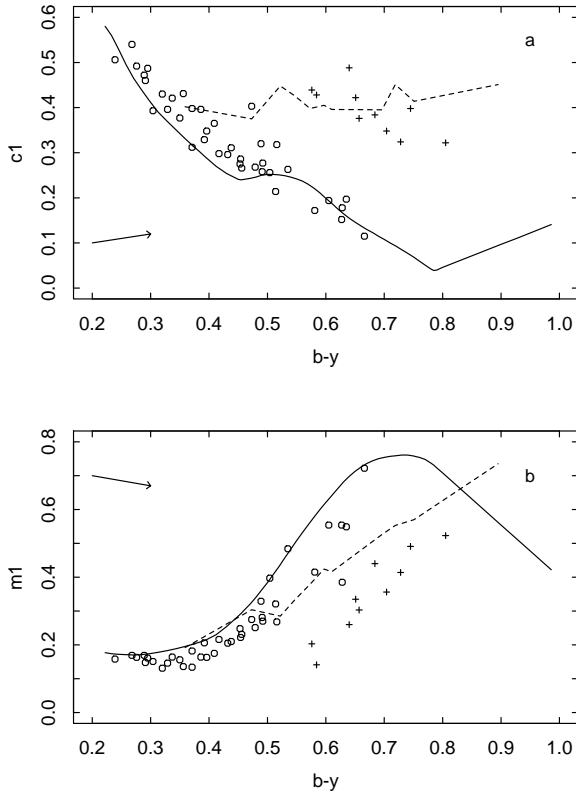


**Fig. 1.** Two-color plots of program stars: **a)**  $c_1$  versus  $(b-y)$ , **b)**  $m_1$  versus  $(b-y)$ . Panel **a)** shows a clear separation among luminosity classes III and V. Pluses indicate stars we classify as giants, while empty symbols indicate main sequence stars. Solid lines indicate the standard main sequence for F (Crawford 1975) and G-M (Olsen 1984) stars. Dashed lines connect data obtained by Perry et al. (1987) for 13 class III stars. Arrows indicate the reddening vector

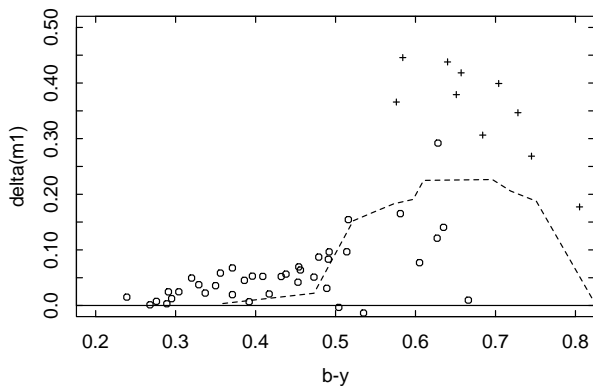


**Fig. 2.**  $\delta m_{1(b-y)}$  versus color for program stars; symbols and lines as in Fig. 1. The dashed line indicates the expected value of  $\delta m_1$  for normal giants

authors find that the observed  $m_1$  anomaly becomes larger in cooler binary systems and that, when individual components are resolved, the metal deficiency implied by the observed  $\delta m_1$  in the cooler, active component is consistently larger than the deficiency implied in the hotter, non-active component. This is incompatible with an effect actually due to anomalous chemical abundances, as the abundance of both binary components, which share a common evolutionary history, is expected to be the same. Giménez et al. (1991) conclude that the observed  $m_1$  index is in fact affected by the chromospheric activity level of the stars, as suggested by their observed relation between the amplitude of magnitude variations (assuming that they are due to the change of spot surface coverage and therefore related to the activity level) and the size of  $\delta m_1$ .

Additional evidence of apparent metal deficiencies induced by stellar activity is present in the literature since some time: the influence of stellar activity on the observed Strömgren photometric indices was already suggested by Giampapa et al. (1979), based on their observations of quiet and active zones on the Sun surface. Active solar regions show lower values of the  $m_1$  index than do quiet solar regions, so that the implied  $[\text{Fe}/\text{H}]$  value is  $\sim 35\%$  lower in active than in quiet regions. Also, a long observational campaign on AB Dor (Jetsu et al. 1990), a very young active K star that shows visual variability probably due to the presence of spots, has shown that AB Dor has a value of the  $m_1$  index lower than expected for a young, close to ZAMS, star. Finally, Basri et al. (1989) compared some photospheric absorption lines in active and quiet stars of the same effective temperature, finding evidence of emission in the cores of these lines, which increased with the level of activity. This emission, by decreasing the equivalent width of the absorption lines, could perhaps mimic the appearance of lower metallicity.

Our data confirm that activity affects Strömgren photometric indices also in non binary systems, at least for stars redder than  $b-y \approx 0.450$ , corresponding approximately to spectral type G8. In Fig. 3 we plot, for the dwarfs in our sample, the observed  $\delta m_1$  versus the activity indicator  $f_X/f_V$ . The  $f_X/f_V$  index is computed in the 0.3–3.5 keV band, from the *Einstein* observations of Gioia et al. (1990) and from our optical photometry. Different symbols indicate stars earlier and later than G8. It is evident that higher values of  $\delta m_1$  are correlated with higher activity levels. Also, the cooler stars show an increase in the apparent metal deficiency with respect to the hotter stars.

The large number of binaries or suspected binaries present in our sample do not behave differently from the single stars in the  $\delta m_{1(b-y)}$  versus  $(f_X/f_V)$  plane, as seen in Fig. 3. Also, while our sample is likely to contain a few unrecognized binaries, they are unlikely the cause of the observed peculiar behavior of the  $m_1$  index: following

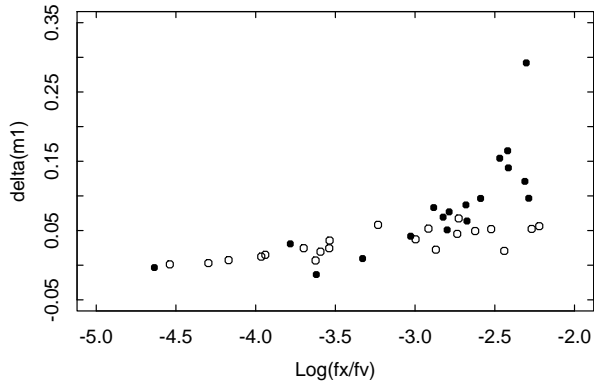


**Fig. 3.**  $\delta m_{1(b-y)}$  versus  $(f_X/f_V)$  for our program stars. Stars earlier and later than G8 are indicated by empty and filled symbols respectively. A clear relation between activity levels and  $m_1$  index deficiency is evident for the cooler stars

the reasoning of Hilditch et al. (1976), Knude (1978) and Giménez et al. (1991), binary systems in which both the components are dwarfs can change their apparent effective temperature by the equivalent of a few spectral subtypes, with all other indices remaining unchanged, while binary systems with at least one evolved component show a  $c_1$  index typical of giants. Therefore the possible presence of unrecognized binaries could not affect  $m_1$  without affecting  $c_1$ .

We have verified that activity does not affect the  $c_1$  index for the stars in our sample (an effect which would make the luminosity class determination unreliable). To this end we have transformed all instrumental colors to the standard colors assuming that all the stars in the sample were main sequence stars, computing for every star the quantities  $\delta c_{1(b-y)} = c_{1(\text{star})} - c_{1(\text{main sequence})}$  for the same color. In the plot of the resulting  $\delta c_{1(b-y)}$  versus  $f_X/f_V$  no clear dependence of  $\delta c_{1(b-y)}$  on activity was found, showing that activity does not affect a star's position in the  $c_1$  vs.  $b-y$  diagram, which can therefore still be used to determine the luminosity class also for very active stars.

The observed anomaly in the observed  $m_1$  indices seems to be exclusively determined by the activity. Let us consider the case of a star similar to the Sun, but completely covered by active regions. If we assume that the observed anomaly in  $m_1$  is due to the filling up of metallic lines in the star's spectrum in the  $v$  band we can write

$$\delta m_1 = m_{1,Q} - m_{1,A} = 2.5 \log\left(\frac{f_A}{f_Q}\right) = 2.5 \log\left(1 + \frac{f_E}{f_Q}\right) \quad (1)$$

where  $m_{1,A}$  is the color index observed in the active star,  $m_{1,Q}$  is the index measured on a quiet star of identical spectral type, and  $f_A$  is the flux emitted in the  $v$  band by the active star, defined as  $f_A = f_E + f_Q$ , where  $f_E$  is the excess flux due to the stellar activity and  $f_Q$  is the flux emitted by the quiet star in the  $v$  band. If we consider the Sun, substituting  $\delta m_1 = 0.027$ , the mean of the Giampapa

et al. (1979) results, we obtain  $f_E/f_Q = 0.025$ , i.e. the chromosphere of a Sun-like stars completely covered by active regions emits, in the  $v$  band, a flux equal to 2.5% of the flux emitted by the photosphere of a quiet star. Let us now consider a K0 star completely covered with active regions similar to those discussed above. In this case we have  $f_Q \sim 0.24 \cdot f_{Q,\odot}$  due to the differences in effective temperature and stellar radius, while  $f_E \sim 0.72 \cdot f_{E,\odot}$  due to the difference in stellar radius only, and assuming that the surface activity flux is independent from spectral type. Hence for a K0 star we can write

$$\delta m_{1,K0} = 2.5 \log\left(1 + \frac{f_{E,K0}}{f_{Q,K0}}\right) = 2.5 \log\left(1 + \frac{0.72 f_{E,\odot}}{0.24 f_{Q,\odot}}\right) \quad (2)$$

With these assumptions we obtain for a K0 star completely covered by active regions a value of  $\delta m_1 = 0.077$ . A similar computation for a K5V star, corresponding approximately to the cooler stars in our sample, yields a maximum value  $\delta m_1 = 0.267$ .

The large  $\delta m_1$  anomaly in the very active, cool stars of our sample (again, implying metallicities comparable to the ones found in halo stars, following the calibration of Olsen 1984), casts some doubts not only on the reliability of the  $m_1$  index for metallicity determinations in populations of unknown characteristics, but also on the usage of Strömgren photometry for the segregation of samples of stars on a population basis.

As discussed earlier, our parent sample has been studied in the past to characterize the presence of an excess of yellow stars in the EMSS (Favata et al. 1993, 1995). These high resolution spectroscopic observations have shown that at least a part of this excess is due to the presence of a young population, at least as measured by the lithium abundance. Similar results have been obtained by other authors on different samples selected, as ours, from X-ray or EUV selected surveys (Tagliaferri et al. 1994; Jeffries et al. 1993; Hodgkin & Pye 1994). In Fig. 4 we show, for the subsample in common with Favata et al. (1993; 1995), a plot of  $\delta m_1$  versus the lithium abundance. The more lithium rich stars are in general the hotter stars (empty symbols in the figure) in which the lithium depletion is slow (Pinsonneault et al. 1990); for these stars no relationship between the  $\delta m_1$  anomaly and the lithium abundance is visible. Instead, for K stars a trend of increasing lithium abundance with increasing  $\delta m_1$  is visible. The three coolest class III stars of Fig. 4 have been classified as probable pre-main sequence stars by Favata et al. (1993) on the basis of their high lithium abundance. We note that in Fig. 4 these stars seem to follow the same trend of the K main sequence stars. For G stars we cannot observe a similar behavior both because the dependence of  $\delta m_1$  on activity indicators is small and because the decay time of the lithium abundance is presumably large with respect of the decay time of activity.



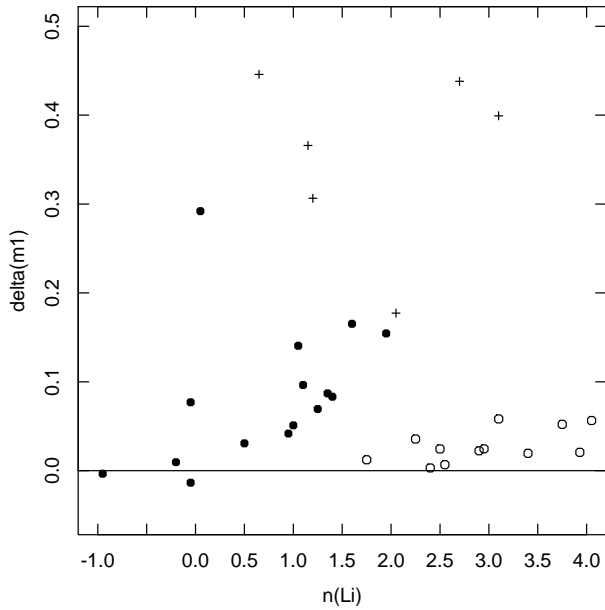


**Fig. 4.**  $\delta m_{1(b-y)}$  versus lithium abundance (in the usual log scale where the hydrogen abundance is set to 12) for program stars. Pluses represent class III stars, empty symbols main sequence stars earlier than G8 and full symbols main sequence stars later than G8. Note as the relationship between  $\delta m_{1(b-y)}$  and lithium abundance for the K stars

In the light of these results and considering that the lithium abundance of K stars is expected to decay very rapidly with increasing age we can conclude that a high lithium abundance is a reliable sign of young age for K stars (see also discussion in Favata et al. 1995). Hence, we have a consistent picture in which the activity in K stars, strictly related with age, affects the  $m_1$  color index in very young active stars.

## 6. Summary and conclusions

We have reported new photometric observations in the Strömgren-Crawford  $wby-\beta$  system of a sample of stars detected in X-ray in the *Einstein* Medium Sensitivity survey. This sample contains an excess of yellow stars with respect to the solar neighborhood stellar population (Favata et al. 1988; Sciortino et al. 1995) attributed to the presence of a young stellar population (Favata et al. 1993, 1995).

Our observations show that stellar positions in the  $c_1$  vs.  $b-y$  diagram are unaffected by activity and that this diagram is still a powerful mean to discriminate between class V and class III stars.

Furthermore main sequence K stars in our sample show values of  $m_1$  index lower respect to those of the Hyades main sequence, mimicking an apparent deficiency of metals. We found that the observed behavior cannot be explained by the presence of unrecognized binaries in the

sample, and that the size of the observed photometric anomaly increases with stellar activity, as measured by the  $f_X/f_V$  ratio, as well as with lithium abundance. Filling-in of the core of metallic lines, due to the high level of activity observed in these stars, is a likely explanation for the  $m_1$  index behavior, making this index unreliable as metallicity indicator for late type stars. The observed dependence of the  $m_1$  anomaly on the lithium abundance is interpreted as an effect induced by the age-dependence of activity level for K stars and the reliable link between high lithium abundance and young age in K dwarfs.

A similar effect is not observed in G stars where the effect of the activity on  $\delta m_1$  seems weak. Data are consistent with a picture in which the chromospheric activity, due to active regions similar to the solar active regions covering up to the overall stellar surface, fill up metallic lines mainly in the  $v$  band. The different behavior of G and K stars is related to the greater ratio  $f_E/f_Q$  between the chromospheric (active) and photospheric (quiet) fluxes in the  $v$  band for K stars with respect to G stars.

**Acknowledgements.** F.M., G.M. and S.S. acknowledge financial support from ASI (Italian Space Agency), MURST (Ministero della Università e della Ricerca Scientifica e Tecnologica), and GNA-CNR. We would like to thank M. Barbera for his contribution in performing the observations. During this work we have extensively used the Simbad database.

## References

- Ardeberg A., Lindgren H., 1981, *Rev. Mexicana. Astron. Astrof.* 6, 173
- Ardeberg A., Lindgren H. 1985, in *Calibration of Fundamental Stellar Quantities*. In: Hayes D.S., Pasinetti L. and Philip A.G.D. (eds.), IAU Symp. 111, 507
- Basri G., Wilcots E., Stout N., 1989, *PASP* 101, 528
- Cayrel de Strobel G., Hauck B., François P., Friel E., Mermillod M., Borde S., 1992, *A&AS* 95, 273
- Crawford D.L., Mander J., 1966, *AJ* 71, 114
- Crawford D.L., Barnes J.V., 1970, *AJ* 75, 978
- Crawford D.L., 1975, *AJ* 80, 955
- Crawford D.L., 1978, *AJ* 83, 48
- Crawford D.L., 1979, *AJ* 84, 1858
- Favata F., Rosner R., Sciortino S., Vaiana G.S., 1988, *ApJ* 324, 1010
- Favata F., Barbera M., Micela G., Sciortino S., 1993, *A&A* 277, 428
- Favata F., Barbera M., Micela G., Sciortino S., 1995, *A&A* 295, 147
- Favata F., Micela G., Sciortino S., 1995, *A&A* 297, L1
- Fleming T.A., Gioia I., Maccacaro T., 1989, *AJ* 98, 692
- Giampapa M.S., Worden S.P., Gilliam L.B., 1979, *ApJ* 229, 1143
- Giménez A., Reglero V., de Castro E., Fernández-Figueroa M.J., 1991, *A&A* 248, 563
- Gioia I., Maccacaro T., Schild R.E., Wolter A., Stocke J.T., 1990, *ApJS* 72, 567
- Gronbeck B., Olsen E.H., Strömgren B., 1976, *A&AS* 26, 155
- Grothues H.G., Gochermann J., 1992, *The Messenger* 68, 43

- Hilditch R.W., Hill G., Barnes J.V., 1976, MNRAS 176, 175  
Hodgkin S.T., Pye J.P., 1994, MNRAS 267, 840  
Jeffries R.D., Bromage G.E., 1993, MNRAS 260, 132  
Jetsu L., Vilhu O., la Dous C., 1990, A&AS 85, 1127  
Knude J., 1978, A&AS 33, 347  
Manfroid J., Heck A., 1983, A&A 120, 302  
Manfroid J., 1992, A&A 271, 714  
McNamara D.H., Powell J.M., 1985, PASP 97, 1101  
Nissen P.E., 1981, A&A 97, 145  
Nissen P.E., Schuster W.J., 1991, A&A 251, 457  
Olsen E.H., 1983, A&AS 54, 55  
Olsen E.H., 1984, A&AS 57, 443  
Olsen E.H., 1988, A&A 189, 173  
Olsen E.H., 1993, A&AS 102, 89  
Olsen E.H., 1994, A&AS 104, 429  
Perry C.L., Olsen E.H., Crawford D.L., 1987, PASP 99, 1184  
Pinsonneault M.H., Kawaler S.D., Demarque P., 1990, ApJS 74, 501  
Pounds K.A., Allan D.J., Barber C., et al., 1993, MNRAS 260, 77  
Reglero V., Giménez A., Estela A., Fabregat J., 1990, Astrophys. Space Sci. 169, 263  
Rufener F., 1986, A&A 165, 275  
Saxner M., Hammarbäck G., 1985, A&A 151, 372  
Schuster W.J., Nissen P.E., 1988, A&A 73, 225  
Schuster W.J., Nissen P.E., 1989, A&A 221, 65  
Schwarz H.E., Melnick J., 1989, The ESO Users Manual 1990, 151  
Sciortino S., Favata F., Micela G., 1995, A&A 296, 370  
Sterken C., Manfroid J., 1992, "Astronomical Photometry - A Guide". Kluwer Academic Publishers, Dordrecht  
Stoeckel J.T., Morris S.L., Gioia I.M., et al., 1991, ApJS 76, 813  
Tagliaferri G., Cutispoto G., Pallavicini R., Randich S., Pasquini L., 1994, A&A 285, 272